Mathematical and Computational Applications

MDPI

Article

Exploring Bifurcation Analysis, Conservation Laws and Soliton Dynamics for the Dual-Mode Nonlinear Schrödinger Equation with Applications

Muhammad Arshad [1,2,3,*], Naila Nasreen [4,5], Evren Hincal [2,6], Mohamed Hafez [7] and Muhammad Farman [2,8,9,*]

1 Department of Mathematics and Statistics, University of Agriculture Faisalabad, Faisalabad 38000, Pakistan
2 Mathematics Research Center, Department of Mathematics, Near East University, Mersin 10, Nicosia 99138, Turkey; evren.hincal@neu.edu.tr
3 Research Center of Applied Mathematics, Khazar University, Baku 1009, Azerbaijan
4 Key Laboratory of High-Efficiency and Clean Mechanical Manufacture (Ministry of Education), School of Mechanical Engineering, Shandong University, Jinan 250061, China; naila_nasreen@hotmail.co.uk
5 Center for Theoretical Physics, Khazar University, 41 Mehseti Str., Baku 1096, Azerbaijan
6 Department of Mathematical Sciences, Saveetha School of Engineering, Saveetha Institute of Medical and Technical Sciences (SIMATS), Chennai 602105, India
7 Faculty of Engineering and Quantity Surviving, INTI International University, Nilai 71800, Malaysia; mohdahmed.hafez@newinti.edu.my
8 Department of Biostatistics and Medical Informatics, Faculty of Medicine, Karadeniz Technical University, Trabzon 61080, Turkey
9 International Center for Interdisciplinary Research in Sciences, The University of Lahore, Lahore 54792, Pakistan
* Correspondence: muhammad.arshad18@yahoo.com (M.A.); farmanlink@gmail.com (M.F.)

Abstract

This study examines the dynamical behavior of the dual-mode nonlinear Schrödinger equation (d-mNLSE), which describes the interaction, amplification, and attenuation of two coexisting wave modes in nonlinear media. The model incorporates key physical parameters including the nonlinearity coefficient, interaction phase velocity, and dispersion parameter, which significantly influence the evolution of nonlinear waves. By applying the modified Sardar sub-equation method (mSS-EM), a wide spectrum of exact analytical solutions is derived. These solutions include mixed trigonometric waves, shock-type structures, singular solutions, complex dark–bright solitons, multi-peak solitons, periodic and mixed-periodic waves, as well as mixed hyperbolic structures. The analytical findings provide useful insight into nonlinear wave propagation phenomena arising in fluid mechanics, water wave dynamics, ocean engineering, and related physical systems. Moreover, the conservation laws of the d-mNLSE are established, which leads to the conserved quantities of impulse power, momentum, and energy and describes the invariant characteristics of the soliton solutions during their propagation. The bifurcation analysis of the reduced dynamical model is carried out to explore the qualitative characteristics of the obtained solutions. The equilibrium points of the considered model are calculated, and their stability properties are analyzed systematically. To demonstrate the physical characteristics of the obtained solutions, different kinds of two-dimensional, three-dimensional, and contour plots are plotted using symbolic computations software. These findings confirm that the analytical method used to obtain the soliton solutions can be used to obtain a variety of soliton solutions of nonlinear evolution equations that appear in applied sciences and engineering.

Keywords: d-mNLSE; mSS-EM; solitons; conservation laws; nonlinear wave propagation; bifurcation analysis

Check for updates

Received: 16 April 2026
Revised: 11 May 2026
Accepted: 28 May 2026
Published: 2 June 2026

Copyright: © 2026 by the authors. Licensee MDPI, Basel, Switzerland. This article is an open access article distributed under the terms and conditions of the Creative Commons Attribution (CC BY) license.

1. Introduction

Nonlinear partial differential equations (NLPDEs) are in a central position in applied mathematics and theoretical physics as they are basic models for a variety of complex phenomena [1–3]. Nonlinear equations capture key characteristics including wave interaction, energy transfer, self-focusing, and pattern generation, in contrast to linear systems [4,5]. Due to these characteristics, NLPDEs are essential for studying biological systems, condensed matter physics, optical communications, fluid dynamics, and plasma physics [6,7]. Specifically, localized structures that form and endure in dispersive media are described by nonlinear wave equations, which provide information on both the qualitative and quantitative aspects of physical processes. For technical and experimental applications, it is therefore not only theoretically interesting but also practically relevant to comprehend the behavior of their solutions [8,9]. Scientists remain highly interested in finding solutions to these types of equations because of their importance in modeling real-life physical phenomena. Due to their significance in describing a variety of physical phenomena and their complex mathematical structure, it is natural that more and more emphasis has been placed on the study of nonlinear PDEs in recent years. Substantial work has been conducted in finding analytical tools for exact solutions and their qualitative analysis in recent decades [10,11]. As a consequence, a variety of reliable tools are now available to find exact solutions of nonlinear evolution equations, providing insight into their qualitative behavior [12,13].

In the nonlinear sciences, dual-mode kind models have recently received a great deal of interest. Because of the fact that novel interactions between the waves are analyzed by the dual-mode equations in the current form, recently, the d-mNLSE received a great deal of interest due to its application to nonlinear wave phenomena, especially in plasma physics and optical fibers. To achieve the exact solutions for the d-mNLSE under various nonlinear conditions, various analytical techniques were developed by the researchers. To describe the possibility of exact and stable solitonic solutions for the d-mNLSE with a parabolic law nonlinearity, analytical soliton solutions were derived for the d-mNLSE [14]. Moreover, the bifurcation pattern and chaotic properties of the d-mNLSE with a power-law nonlinearity were analyzed by Omar and Murad [15]. The authors in [16] obtained exact solutions and studied the bifurcations of the dynamical system resulting from the d-mNLSE. Furthermore, Lie symmetry analysis, group-invariant solutions, and conservation laws of the d-mNLSE were examined in [17]. Moreover, the authors of [18] analyzed a novel extension of the NLSE by utilizing dual-mode optical waves. Apart from the analysis of the effects of dual-mode interactions and third-order dispersion effects, the authors demonstrated the propagation characteristics of the dual-mode waves. In the study conducted by the researchers in [19], the authors investigated the impact of various nonlinear interactions on the propagation of solitons in a dual-mode resonant NLSE. According to the authors of [19], the study showed the interaction of the phase velocity, nonlinearity, and other factors on the propagation of optical solitons. Thus, all the papers discussed above provide a better knowledge of the dual-mode nonlinear dynamics and the basic understandings of the complex wave systems governed by the d-mNLSE.

Moreover, Biswas and other authors employed the tanh-coth expansion approach to arrive at the dual-mode optical soliton solutions of the dual-mode type model in the study conducted in [20]. Wazwaz [21] used a reduced version of Hirota's approach to obtain multiple kink results for the dual-mode Sharma–Tasso–Olver and fourth-order Burgers models. The researchers in [22] used the $\exp(-\phi)$-expansion scheme to develop dual-wave soliton results for dual-mode resonance NLSE. By utilizing the tanh-coth, the unified Riccati equation, and the novel extended auxiliary equation methods, Zayed and Shohib [23] were able to obtain several families of Jacobi elliptic results, dark, singular, solitary waves, and

other wave results. The dual-mode Korteweg–de Vries equation is the subject of several previous publications [24–26].

Extensive investigations have been carried out on bifurcation analysis and the construction of exact wave results for NLPDEs. Chaos, a hallmark of nonlinear systems, is widely observed across various scientific disciplines [27]. Conservation laws (CLs) also play an essential role in characterizing the behavior of mechanical, electrical, optical, chemical, biological, and atmospheric systems. Despite their differing physical origins, such systems frequently display comparable qualitative and quantitative dynamics, often resulting from the breakdown of periodic motion. Additionally, sensitivity analysis has become an essential tool to understand the effect of changes in the parameters on the output of the model with increased accuracy and minimum prediction uncertainties [28–30].

In the present study, the mSS-EM is employed to find the analytical soliton solutions to the d-mNLSE. This approach is more appropriate to solve nonlinear evolution equations with both linear and nonlinear interactions. This allows us to find diverse exact solutions with respect to other analytical techniques. Moreover, the conservation laws are obtained to find the important invariants such as the power, momentum, and energy of the soliton with respect to the d-mNLSE. In addition, bifurcation analysis is carried out to investigate the qualitative behavior of the reduced dynamical system and the stability characteristics of the equilibrium states.

This remaining paper is organized as follows: In Section 2, the theoretical background of the mSS-EM method is given. Section 3 is focused on the derivation of the dynamical model of the d-mNLSE. Then, the application of the presented method to the dynamical model of the d-mNLSE for the derivation of the analytical soliton solutions is given in Section 4. Section 5 is devoted to the derivation and discussion of the conservation laws associated with the model. Moreover, the qualitative analysis of the dynamical model of the d-mNLSE is given through the bifurcation analysis in Section 6. Then, the physical interpretation of the obtained solutions is provided in Section 7. Finally, the main results of the paper are summarized in Section 8.

2. Description of Method

The SS-EM is enhanced by incorporating additional terms and parameters into the trial function, thereby extending its capability to handle a broader class of nonlinear partial differential equations. This improved approach has been successfully applied to numerous NLPDEs arising in mathematics and physics. Considering the general form of NLPDEs

$$F(Q, Q_t, Q_x, Q_{tt}, Q_{tx}, Q_{xx}, \ldots) = 0, \tag{1}$$

where $Q = Q(x,t)$ is real value function of x and t, the main stages of mSS-EM are as follows.

Step 1: Consider the transformation of traveling wave as

$$Q(x,t) = U(\zeta), \zeta = \alpha x - \omega t + \theta, \tag{2}$$

where α and ω are wave number and frequency while θ is real constant. Inserting Equations (2) into (1) yields a NLODE as

$$G\Big(U, -\omega U', \alpha U', \omega^2 U'', -\alpha\omega U'', \ldots\Big) = 0. \tag{3}$$

Step 2: Assume the general solution of above equation has the kind as

$$U(\zeta) = \sum_{k=0}^{N} A_k \Psi^k(\zeta), A_k \neq 0, \tag{4}$$

where Ψ promises the following ODE:

$$\left(\Psi'(\zeta)\right)^2 = \mu_1 + \mu_2 \Psi^2(\zeta) + \mu_3 \Psi^4(\zeta), \tag{5}$$

where $\mu_1 \neq 1, \mu_2, \mu_3 \neq 0$ are integers, constants $A_k (k = 0, \pm 1, \pm 2, \ldots, \pm N)$ are real. Intiger N is assessed by utilizing the balancing principle.

Step 3: After substitution, the subsequent polynomial is expressed in terms of powers of $\Psi^k \Psi'$ by combining Equations (4) and (5) into (3).

Step 4: An algebraic system is articulated for the unknown parameters A_k, β, μ_1, μ_2, μ_3, ω, etc., by setting to zero the coefficients of all distinct coefficients of Ψ.

Step 5: Finally, the parameter values are determined by solving the resulting algebraic system with the aid of Mathematica. The achieved results are then incorporated into Equation (4) to construct the results of Equation (1).

3. Governing Dynamical Model

In this article, the dual-mode equations are analyzed in detail. These structures describe the simultaneous wave interactions between two distinct modes. The dual-mode form of the Korteweg–de Vries equation is presented as follows [31]:

$$Q_{tt} - c^2 Q_{xx} + \left(\frac{\partial}{\partial t} - \lambda c \frac{\partial}{\partial x}\right) Q Q_x + \left(\frac{\partial}{\partial t} - c\epsilon \frac{\partial}{\partial x}\right) Q_{xxx} = 0, \tag{6}$$

where $Q(x,t)$ denotes the complex field amplitude, x and t represent the spatial and temporal variables, respectively. The parameter $c \geq 0$ corresponds to the interaction phase velocity, $\lambda \leq \pm 1$ characterizes the nonlinearity, and $\epsilon \leq \pm 1$ denotes the dispersive effect.

Equation (6) represents the d-mKdV equation. It designates the interaction (collision) of waves in the presence of different dispersive effects, similar to the Hirota–Satsuma model [32].

Equation (6) reduces to the standard KdV model by setting $c = 0$. Furthermore, integrating with respect to t yields

$$Q_t + Q Q_x + Q_{xxx} = 0. \tag{7}$$

Let us consider the below equation:

$$Q_t + N(Q, Q_x, \ldots) + L(Q_{xx}, Q_{xxx}, \ldots) = 0, \tag{8}$$

where the second and third terms represent the linear and nonlinear operators, respectively, which are extended to obtain the dual-mode version as follows:

$$Q_{tt} - c^2 Q_{xx} + \left(\frac{\partial}{\partial t} - \lambda c \frac{\partial}{\partial x}\right) N(Q, Q_x, \ldots) + \left(\frac{\partial}{\partial t} - c\epsilon \frac{\partial}{\partial x}\right) L(Q_{xx}, Q_{xxx}, \ldots) = 0. \tag{9}$$

We consider the NLSE as

$$i Q_t + \frac{Q_{xx}}{2} + F\left(|Q|^2\right) Q = 0, \tag{10}$$

where F and Q denote the functions of envelope and the classical form of the nonlinear, respectively. Utilizing Equations (8) and (9), the d-mNLSE is attained as follows [33]:

$$i\left(Q_{tt} - c^2 Q_{xx}\right) + \left(\frac{\partial}{\partial t} - c\lambda \frac{\partial}{\partial x}\right)\left(F\left(|Q|^2\right) Q\right) + \left(\frac{\partial}{\partial t} - c\epsilon \frac{\partial}{\partial x}\right) \frac{Q_{xx}}{2} = 0. \tag{11}$$

4. Soliton Formation

We now apply the mSS-EM to the d-mNLSE with a cubic nonlinearity. Under the cubic law, $F(Q) = Q$, and consequently Equation (11), reduces to the following form:

$$i\Big(Q_{tt} - c^2 Q_{xx}\Big) + \left(\frac{\partial}{\partial t} - c\lambda\frac{\partial}{\partial x}\right)\Big(|Q|^2 Q\Big) + \left(\frac{\partial}{\partial t} - c\epsilon\frac{\partial}{\partial x}\right)\frac{Q_{xx}}{2} = 0. \tag{12}$$

Since Equation (12) is a complex-valued equation, we introduce the following traveling-wave transformation:

$$Q(x,t) = \Psi(\zeta)e^{i\kappa},\ \ \zeta = \alpha x - \omega t + \theta,\ \ \kappa = \beta x - \nu t, \tag{13}$$

where α, β and ν, ω are wave numbers and frequencies of waves, respectively. Deputizing Equations (13) into (12) and splitting the real and imaginary segments, we obtain the bellowing NLODEs as

$$\Big(\alpha^2\nu + 2\alpha\beta\omega + 2\alpha^2c^2 + 3\alpha^2\beta c\epsilon - 2\omega^2\Big)\Psi'' + \Big(2\nu^2 - \beta^2\nu - 2\beta^2c^2 - \beta^3c\epsilon\Big)\Psi + 2(\beta c\lambda + \nu)\Psi^3 = 0. \tag{14}$$

and

$$-\alpha^2(\alpha c\epsilon + \omega)\Psi''' + \Big(2\alpha\beta\nu + \beta^2\omega + 4\alpha\beta c^2 + 3\alpha\beta^2c\epsilon - 4\nu\omega - 6(\alpha c\lambda + \omega)\Psi^2\Big)\Psi' = 0. \tag{15}$$

Integrating the above Equation (15) with respect to ζ and setting the constant of integration to zero yields

$$\alpha^2(\alpha c\epsilon + \omega)\Psi'' - \Big(2\alpha\beta\nu + \beta^2\omega + 4\alpha\beta c^2 + 3\alpha\beta^2c\epsilon - 4\nu\omega\Big)\Psi + 2(\alpha c\lambda + \omega)\Psi^3 = 0. \tag{16}$$

As Equations (14) and (16) are similar, the relationships between the coefficients are obtained as

$$\lambda = \epsilon = -\frac{\omega}{\alpha c}, \nu = \frac{\beta(\beta\omega - 2\alpha c^2)}{\alpha\beta - 2\omega}. \tag{17}$$

Utilizing the homogeneous balancing principle to Equation (14) gives $N = 1$, and we assume the solution of Equation (14) in the form

$$\Psi(\zeta) = \frac{A_{-1}}{\Psi(\zeta)} + A_0 + A_1\Psi(\zeta). \tag{18}$$

Putting Equations (18) along with (5) into Equation (14) and equating to zero the coefficients of $\Psi^i\Psi^{(j)}$, we obtain a system of equations for the parameters $A_{-1}, A_0, A_1, \mu_1, \mu_2, \mu_3$, $\alpha, \beta, \omega, \nu, \theta, \lambda, c$ and ϵ. This system of equations is solved via Mathematica 10.3, and the below sets of solution are obtained:

$$A_{-1} = 0, A_0 = 0, A_1 = \sqrt{-\frac{2\alpha\mu_3\omega}{\beta}}, c = \frac{\sqrt{\alpha^2\beta\mu_2\omega - 2\alpha\mu_2\omega^2 + \beta^3\omega}}{\sqrt{2\alpha}\beta}. \tag{19}$$

Using the solution set given in Equation (19), we derive the families of wave results as follows.

Family 1: If $\mu_1 = 0, \mu_2 > 0$ and $\mu_3 \neq 0$, then

$$Q_1^1(x,t) = \sqrt{\frac{2\alpha\mu_2\omega}{\beta}}\,\mathrm{sech}(\sqrt{\mu_2}(\zeta + \zeta_0))e^{i\kappa}. \tag{20}$$

Figure 1 exhibits graphical representation of the solution in Equation (20).

$$Q_1^2(x,t) = \sqrt{\frac{2\alpha\mu_2\omega}{\beta}}\operatorname{csch}(\sqrt{\mu_2}(\zeta+\zeta_0))e^{i\kappa}. \tag{21}$$

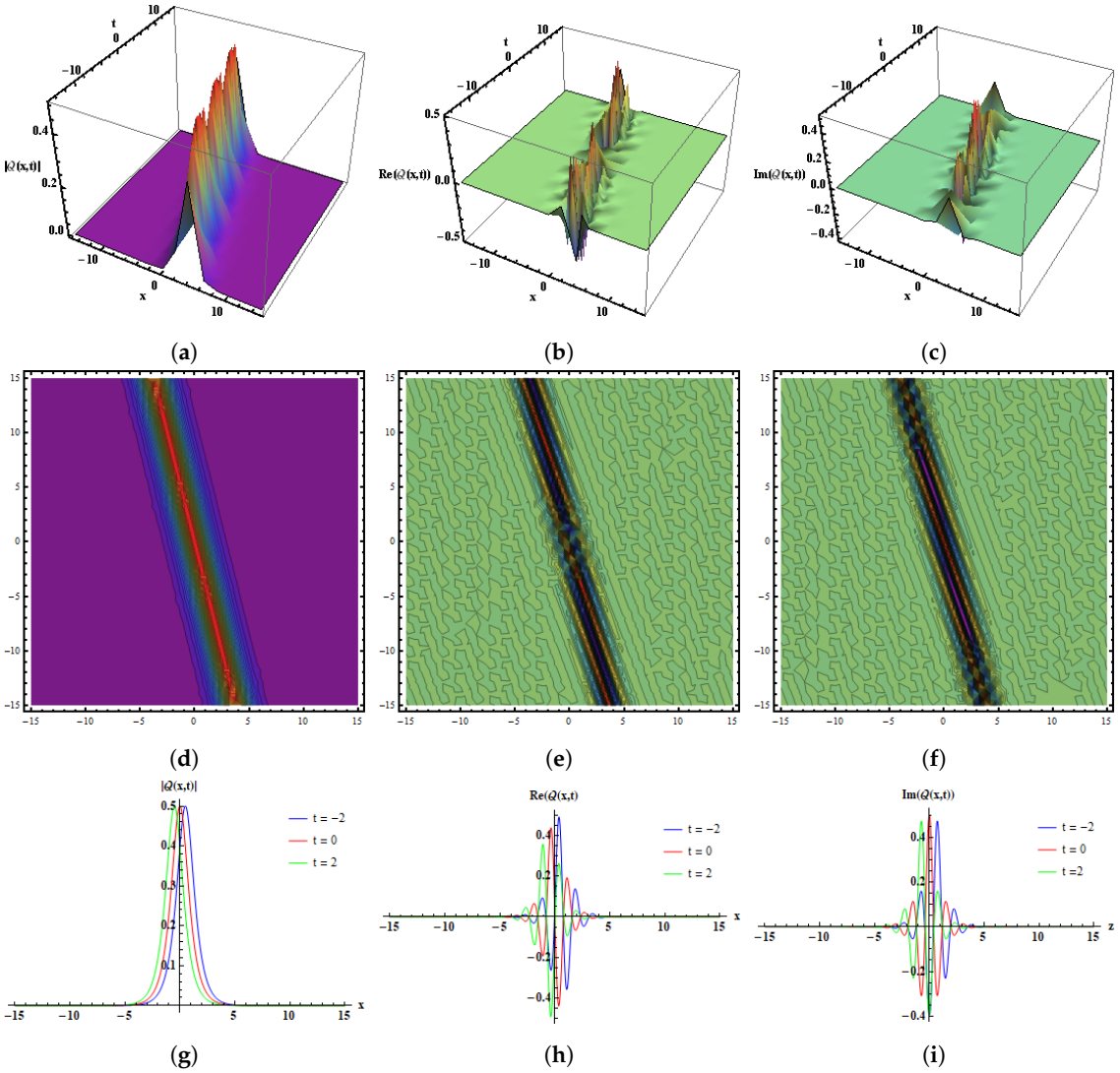


Figure 1. Diverse wave structures corresponding to solution in Equation (20) are depicted at $\alpha = 2$, $\beta = 4$, $\mu_2 = \mu_3 = 0.5$, $\nu = -1.5$, $\tau = 1$, $\omega = -0.5$ as (**a**) bright soliton, (**b**,**c**) breather-type wave structures with corresponding contourplots (CPs) (**d**–**f**) and two-dimensional (2D) surface views (**g**–**i**).

Family 2: For constants k_1 and k_2, let $\mu_1 = 0, \mu_2 > 0$ and $\mu_3 = 4k_1k_2$, then

$$Q_2^1(x,t) = \frac{\sqrt{-8\alpha k_1k_2\mu_2\omega}}{\sqrt{\beta}(k_1-k_2)\left(\sinh\left(\sqrt{\mu_2}(\zeta+\zeta_0)\right)+\cosh\left(\sqrt{\mu_2}(\zeta+\zeta_0)\right)\right)}e^{i\kappa}. \tag{22}$$

Family 3: For constants E_1 and E_2, let $\mu_1 = \frac{\mu_2^2}{4\mu_3}$, $\mu_2 < 0$ and $\mu_3 > 0$, then

$$Q_3^1(x,t) = \sqrt{\frac{\alpha\mu_2\omega}{\beta}}\tanh\left(\frac{\sqrt{-\mu_2}(\zeta+\zeta_0)}{\sqrt{2}}\right)e^{i\kappa}. \tag{23}$$

Figure 2 exhibits graphical representation of the solution in Equation (23).

$$Q_3^2(x,t) = \sqrt{\frac{\alpha\mu_2\omega}{\beta}}\coth\left(\frac{\sqrt{-\mu_2}(\zeta+\zeta_0)}{\sqrt{2}}\right)e^{i\kappa}. \tag{24}$$

$$Q_3^3(x,t) = \sqrt{\frac{\alpha\mu_2\omega}{\beta}}\left(\tanh\left(\frac{\sqrt{-\mu_2}(\zeta+\zeta_0)}{\sqrt{2}}\right)+i\,\mathrm{sech}\left(\sqrt{-2\mu_2}(\zeta+\zeta_0)\right)\right)e^{i\kappa}. \tag{25}$$

Figure 3 exhibits graphical representation of the solution in Equation (25).

$$Q_3^4(x,t) = \sqrt{\frac{\alpha\mu_2\omega}{4\beta}}\left(\tanh\left(\frac{\sqrt{-\mu_2}(\zeta+\zeta_0)}{2\sqrt{2}}\right)+\coth\left(\frac{\sqrt{-\mu_2}(\zeta+\zeta_0)}{2\sqrt{2}}\right)\right)e^{i\kappa}. \tag{26}$$

$$Q_3^5(x,t) = \frac{\sqrt{\frac{\alpha\mu_2\omega}{\beta}}\cosh\left(\sqrt{-2\mu_2}(\zeta+\zeta_0)\right)}{\sinh\left(\sqrt{-2\mu_2}(\zeta+\zeta_0)\right)+i}e^{i\kappa}. \tag{27}$$

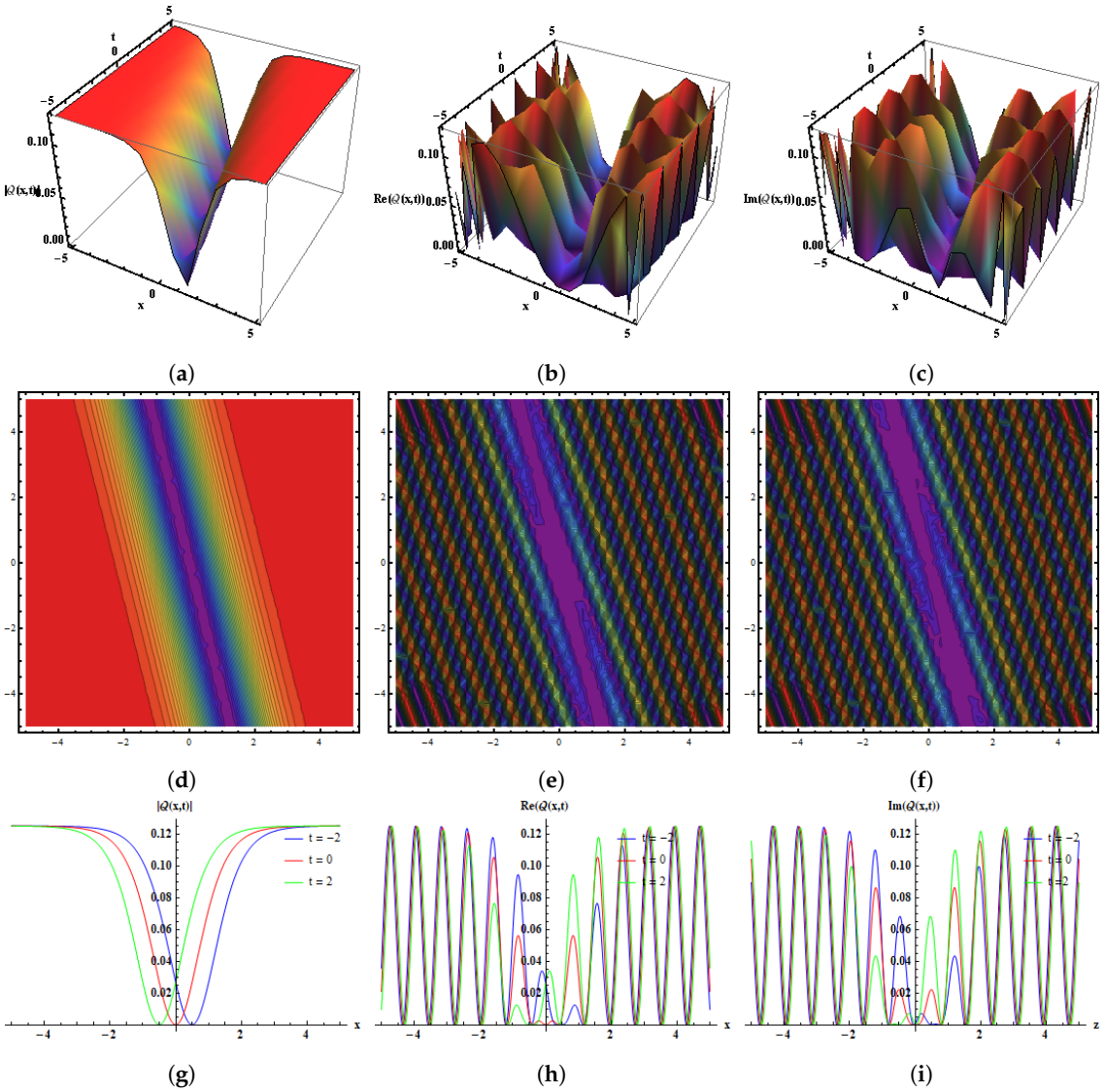


Figure 2. Illustration of the solution in Equation (23) in diverse forms at $\alpha = 2, \mu_2 = -0.5, \mu_3 = 0.5, \beta = 4, \theta = -1, \nu = -1.5, \tau = 1, \omega = -0.5$ as (**a**) dark soliton, (**b**,**c**) dark-type periodic wave structures with corresponding CPs (**d**–**f**) and 2D surface views (**g**–**i**).

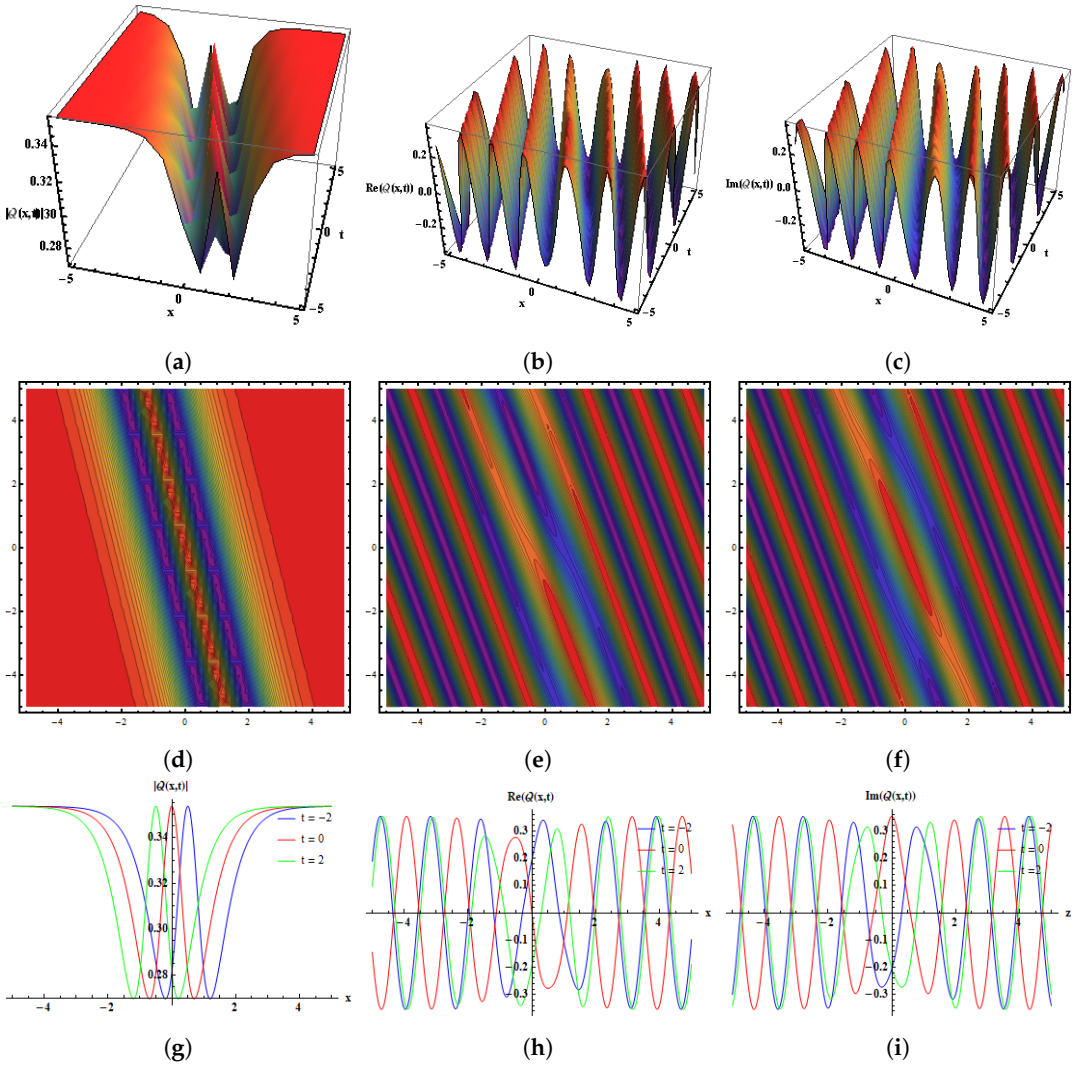


Figure 3. Diverse wave structures corresponding to solution in Equation (25) are depicted at $\alpha = 2$, $\beta = 4, \theta = -1, \mu_2 = -0.5, \mu_3 = 0.5, \nu = -1.5, \tau = 1, \omega = -0.5$ as (**a**) W-shape soliton, (**b**,**c**) periodic wave structures with corresponding CPs (**d**–**f**) and 2D surface views (**g**–**i**).

Family 4: Let $\mu_1 = 0, \mu_2 < 0$ and $\mu_3 = 0$, then

$$Q_4^1(x,t) = \sqrt{\frac{2\alpha\mu_2\omega}{\beta}}\,\sec\left(\sqrt{-\mu_2}(\zeta+\zeta_0)\right)e^{i\kappa}. \tag{28}$$

Figure 4 exhibits graphical representation of the solution in Equation (28).

$$Q_4^2(x,t) = \sqrt{\frac{2\alpha\mu_2\omega}{\beta}}\,\csc\left(\sqrt{-\mu_2}(\zeta+\zeta_0)\right)e^{i\kappa}. \tag{29}$$

Family 5: Let $\mu_1 = \frac{\mu_2^2}{4\mu_3}$, $\mu_2 > 0$ and $\mu_3 > 0$ and $E_1^2 - E_2^2 > 0$, then

$$Q_5^1(x,t) = \sqrt{\frac{\alpha\mu_2\omega}{\beta}}\,\tan\left(\frac{\sqrt{\mu_2}(\zeta+\zeta_0)}{\sqrt{2}}\right)e^{i\kappa}. \tag{30}$$

Figure 5 exhibits graphical representation of the solution in Equation (30).

$$Q_5^2(x,t) = -\sqrt{\frac{\alpha\mu_2\omega}{\beta}}\,\cot\left(\frac{\sqrt{\mu_2}(\zeta+\zeta_0)}{\sqrt{2}}\right)e^{i\kappa}. \tag{31}$$

$$Q_5^3(x,t) = \sqrt{\frac{\alpha\mu_2\omega}{\beta}}\left(\sec\left(\sqrt{2\mu_2}(\zeta+\zeta_0)\right) - \tan\left(\sqrt{2\mu_2}(\zeta+\zeta_0)\right)\right)e^{i\kappa}. \tag{32}$$

$$Q_5^4(x,t) = \sqrt{\frac{\alpha\mu_2\omega}{4\beta}}\left(\tan\left(\frac{\sqrt{\mu_2}(\zeta+\zeta_0)}{2\sqrt{2}}\right) - \cot\left(\frac{\sqrt{\mu_2}(\zeta+\zeta_0)}{2\sqrt{2}}\right)\right)e^{i\kappa}. \tag{33}$$

$$Q_5^5(x,t) = \sqrt{\frac{\alpha\mu_2\omega}{\beta}}\frac{\left(\sqrt{E_1^2-E_2^2} - E_1\cos\left(\sqrt{2\mu_2}(\zeta+\zeta_0)\right)\right)}{E_1\sin\left(\sqrt{2\mu_2}(\zeta+\zeta_0)\right)+E_2}e^{i\kappa}. \tag{34}$$

$$Q_5^6(x,t) = \sqrt{\frac{\alpha\mu_2\omega}{\beta}}\frac{\cos\left(\sqrt{2\mu_2}(\zeta+\zeta_0)\right)}{\sin\left(\sqrt{2\mu_2}(\zeta+\zeta_0)\right)-1}e^{i\kappa}. \tag{35}$$

Family 6: Let $\mu_1 = 0$ and $\mu_2 > 0$, then

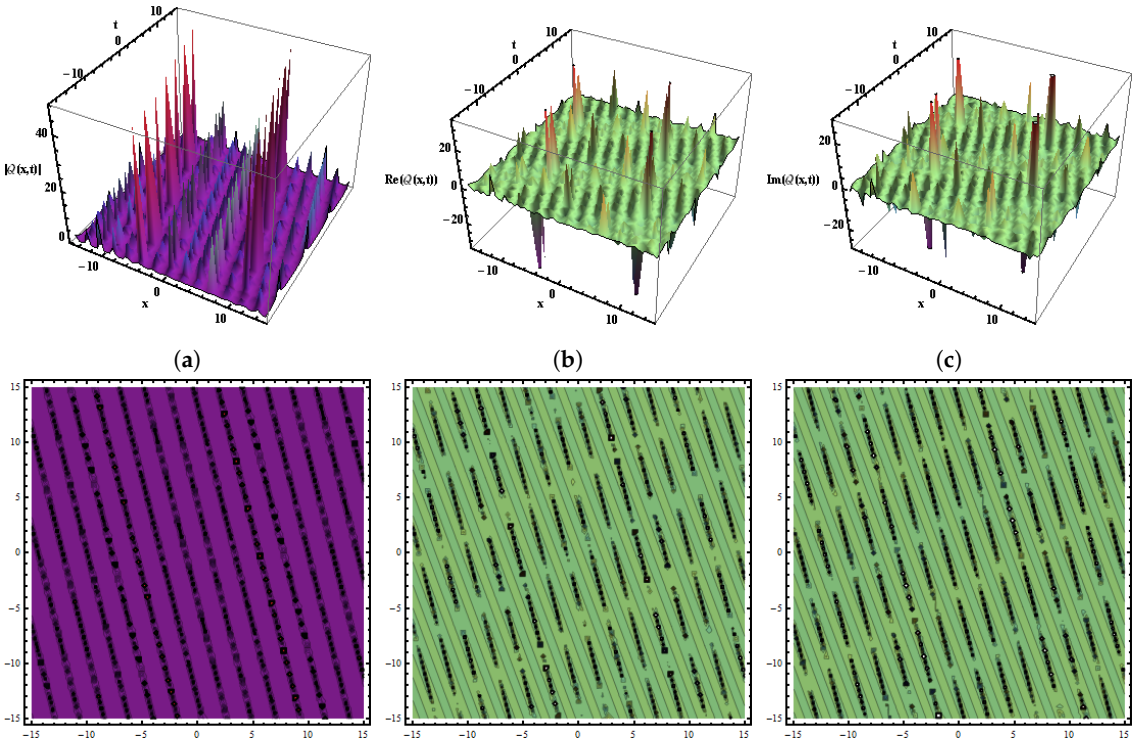
$$Q_6^1(x,t) = \sqrt{-\frac{2\alpha\mu_3\omega}{\beta}}\frac{\left(4\mu_2 e^{\sqrt{\mu_2}(\zeta+\zeta_0)}\right)}{e^{2\sqrt{\mu_2}(\zeta+\zeta_0)} - 4\mu_2\mu_3}e^{i\kappa}. \tag{36}$$

$$Q_6^2(x,t) = \sqrt{-\frac{2\alpha\mu_3\omega}{\beta}}\frac{4\mu_2 e^{\sqrt{\mu_2}(\zeta+\zeta_0)}}{1-4\mu_2\mu_3 e^{2\sqrt{\mu_2}(\zeta+\zeta_0)}}e^{i\kappa}. \tag{37}$$

Family 7: Let $\mu_1 = 0, \mu_2 = 0$ and $\mu_3 > 0$, then

$$Q_7^1(x,t) = \sqrt{-\frac{2\alpha\omega}{\beta}}\frac{1}{\zeta+\zeta_0}e^{i\kappa}. \tag{38}$$

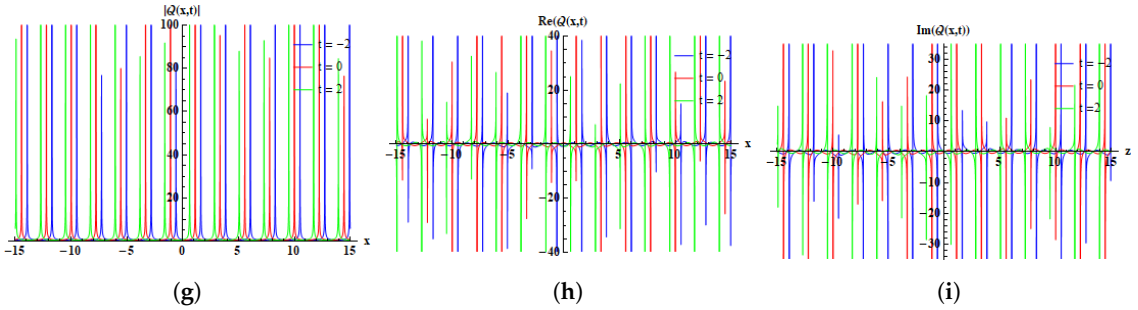
$$Q_7^2(x,t) = \frac{\sqrt{2\alpha\omega}}{\sqrt{\beta}(\xi+\tau)}e^{i\kappa}. \tag{39}$$



(**a**) (**b**) (**c**)

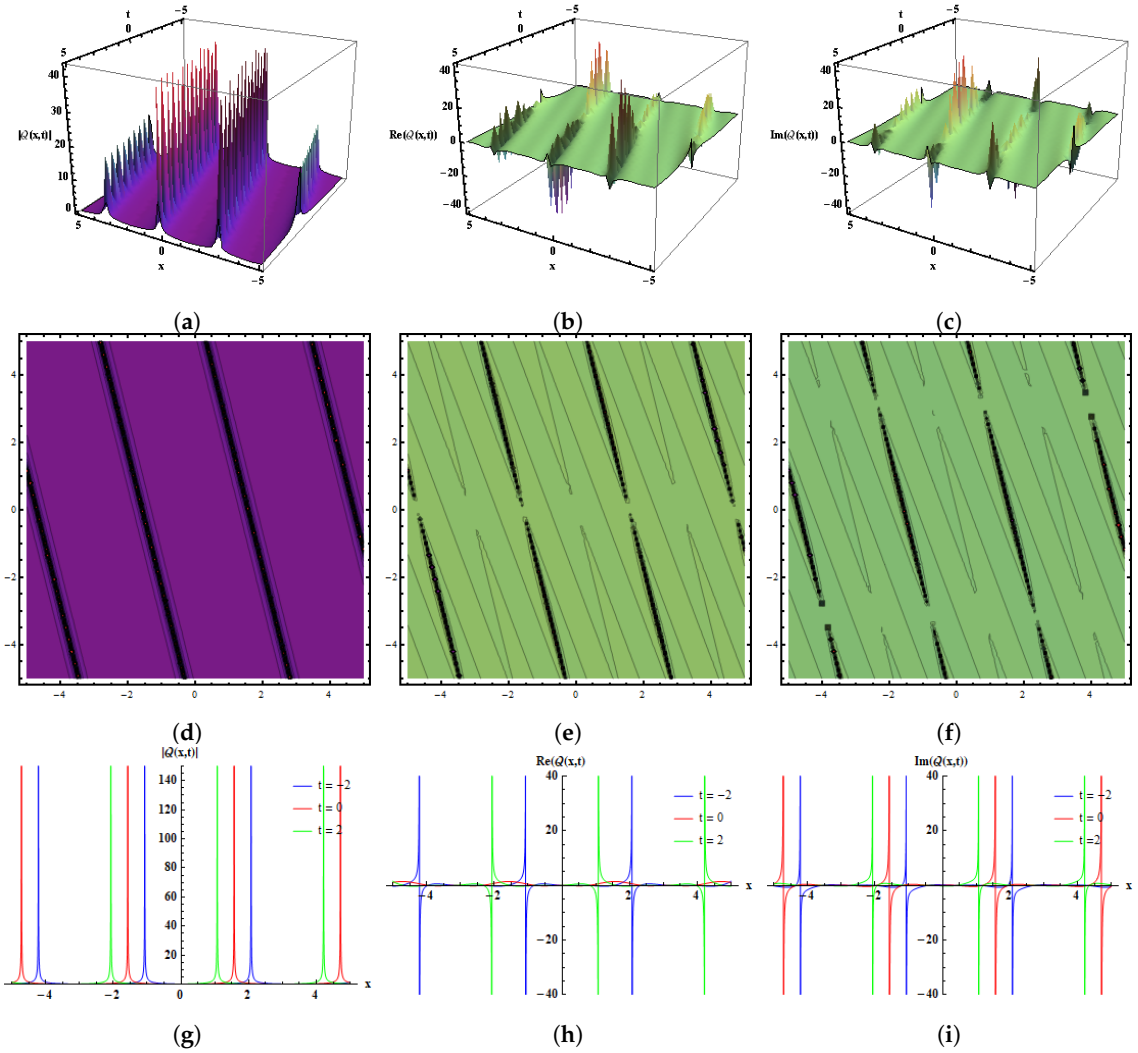
(**d**) (**e**) (**f**)

Figure 4. *Cont.*



(**g**) (**h**) (**i**)

Figure 4. Illustration of the solution in Equation (28) in diverse forms at $\alpha = 2, \beta = 4, \omega = \mu_2 = -0.5$, $\mu_3 = 0.5, \theta = \nu = -1.5, \tau = 1$ as (**a**) Multi-peak solitons of diverse amplitudes, (**b**,**c**) breather-type interactional wave structures with corresponding CPs (**d**–**f**) and 2D surface views (**g**–**i**).



(**a**) (**b**) (**c**)

(**d**) (**e**) (**f**)

(**g**) (**h**) (**i**)

Figure 5. Illustration of the solution in Equation (30) in diverse forms at $\alpha = 2, \beta = 4, \mu_2 = \mu_3 = 0.5$, $\nu = -1.5, \theta = \tau = 1, \omega = -0.5$ as (**a**) periodic multi-peak solitons of diverse amplitudes, (**b**,**c**) breather-type wave structures with corresponding CPs (**d**–**f**) and 2D surface views (**g**–**i**).

5. Conservation Laws

In this section, we present a detailed analysis of the CLs associated with the d-mNLSE described in Equation (12). CLs play an important role in understanding the physical properties and invariant quantities of nonlinear wave systems. They provide insight into how key quantities remain preserved during the evolution of the wave field. By deriving these conserved quantities, we highlight important structural characteristics of

the governing equation and its dynamical behavior. These results also help explain the stability and propagation features of nonlinear waves described by the model.

5.1. First CL

To derive the first CL for Equation (12), we perform a direct calculation.

$$i\Big(Q_{tt} - c^2 Q_{xx}\Big) + \left(\frac{\partial}{\partial_t} - \lambda c\frac{\partial}{\partial_x}\right)\Big((|Q|)^2 Q\Big) + \left(\frac{\partial}{\partial_t} - \epsilon c\frac{\partial}{\partial_x}\right)\frac{Q_{xx}}{2} = 0. \tag{40}$$

We expand the differential operator in the above equation and then write the resulting equation in total derivative form as

$$i\frac{\partial}{\partial t}Q_t - ic^2\frac{\partial}{\partial x}Q_x + \frac{\partial}{\partial t}\Big(|Q|^2 Q\Big) - \lambda c\frac{\partial}{\partial x}\Big(|Q|^2 Q\Big) + \frac{\partial}{\partial t}\left(\frac{Q_{xx}}{2}\right) - \epsilon c\frac{\partial}{\partial x}\left(\frac{Q_{xx}}{2}\right) = 0. \tag{41}$$

The above can also be written as

$$i\frac{\partial}{\partial t}\left(iQ_t + |Q|^2 Q + \frac{Q_{xx}}{2}\right) - \frac{\partial}{\partial x}\left(ic^2 Q_x + \lambda c|Q|^2 Q + \epsilon c\frac{Q_{xx}}{2}\right) = 0. \tag{42}$$

The above Equation (42) can be rewritten in the form of a CL as follows:

$$\frac{\partial T}{\partial t} + \frac{\partial J}{\partial x} = 0, \tag{43}$$

here, T and J are as

$$T = iQ_t + (|Q|)^2 Q + \frac{Q_{xx}}{2}),$$
$$\text{and } J = ic^2 Q_x + \lambda c\Big((|Q|)^2 Q\Big) + \epsilon c\frac{Q_{xx}}{2}.$$

From Equation (43), the corresponding conserved quantity can be obtained and written as follows:

$$P = \int_{-\infty}^{\infty} T dx = \int_{-\infty}^{\infty}\left(iQ_t + (|Q|)^2 Q + \frac{Q_{xx}}{2}\right)dx. \tag{44}$$

The above conservative quantity represents the impulse power of the solitons. This conserved quantity proves that the impulse energy of the derived solitons is invariant during their transmission in the nonlinear dispersive environment.

5.2. Second Conservation Law

We multiply Equation (12) by Q^* and conjugate it by Q, then adding yield as

$$\begin{aligned} &i(Q^* Q_{tt} - QQ^*_{tt}) + ic^2(QQ^*_{xx} - Q^* Q_{xx}) + Q^*\frac{\partial}{\partial t}\Big(|Q|^2 Q\Big) + Q\frac{\partial}{\partial t}\Big(|Q|^2 Q^*\Big) \\ &- c\lambda\left(Q^*\frac{\partial}{\partial x}\Big(|Q|^2 Q\Big) + Q\frac{\partial}{\partial x}\Big(|Q|^2 Q^*\Big)\right) \\ &+ \frac{1}{2}(Q^* Q_{xxt} + QQ^*_{xxt}) - \frac{c\epsilon}{2}(Q^* Q_{xxx} + QQ^*_{xxx}) = 0. \end{aligned} \tag{45}$$

By using the identity, the above equation can be written as

$$\begin{aligned} &i\frac{\partial}{\partial t}(Q^* Q_t - QQ^*_t) + ic^2\frac{\partial}{\partial x}(QQ^*_x - Q^* Q_x) + \frac{3}{2}\frac{\partial|Q|^4}{\partial t} - \frac{3c\lambda}{2}\frac{\partial|Q|^4}{\partial x} + \frac{1}{2}\frac{\partial}{\partial t}(Q^* Q_{xx} + QQ^*_{xx}) \\ &- \frac{1}{2}\frac{\partial}{\partial x}(Q^*_t Q_x + Q_t Q^*_x) - \frac{1}{2}\frac{\partial}{\partial t}\Big(|Q_x|^2\Big) - \frac{c\epsilon}{2}\frac{\partial}{\partial x}(Q^* Q_{xx} + QQ^*_{xx}) + \frac{c\epsilon}{4}\frac{\partial}{\partial x}\Big(|Q_x|^2\Big) = 0. \end{aligned} \tag{46}$$

The above equation can be written in conservation law form as

$$\frac{\partial T}{\partial t} + \frac{\partial J}{\partial x} = 0, \tag{47}$$

where T and J take the form

$$T = i(Q^*Q_t - QQ_t^*) + \frac{3}{2}|Q|^4 + \frac{1}{2}(Q^*Q_{xx} + QQ_{xx}^*) + \frac{1}{2}|Q_x|^2,$$
$$\text{and } J = ic^2(QQ_x^* - Q^*Q_x) - \frac{3c\lambda}{2}|Q|^4 - \frac{1}{2}(Q_t^*Q_x + Q_tQ_x^*) - \frac{c\epsilon}{2}(Q^*Q_{xx} + QQ_{xx}^*) + \frac{c\epsilon}{4}|Q_x|^2.$$

The conserved quantity of momentum is attained as

$$M = \int_{-\infty}^{\infty}\left(i(Q^*Q_t - QQ_t^*) + \frac{3}{2}|Q|^4 + \frac{1}{2}(Q^*Q_{xx} + QQ_{xx}^*) + \frac{1}{2}|Q_x|^2\right)dx = cons, \tag{48}$$

which is corresponding to momentum of solitons. The conservation of momentum shows that the wave profile is stable and consistent when subjected to dual-mode interactions.

5.3. Third CL

To derive the third CL, multiplying Equation (12) by Q_t^* and its complex conjugate by Q_t, and subtracting the subsequent phrases, we get

$$\begin{aligned} &i(Q_t^*Q_{tt} + Q_tQ_{tt}^*) - ic^2(Q_t^*Q_{xx} + Q_tQ_{xx}^*) + Q_t^*\frac{\partial}{\partial t}\left(|Q|^2Q\right) - Q_t\frac{\partial}{\partial t}\left(|Q|^2Q^*\right) \\ &- c\lambda\left(Q_t^*\frac{\partial}{\partial x}\left(|Q|^2Q\right) - Q_t\frac{\partial}{\partial x}\left(|Q|^2Q^*\right)\right) \\ &+ \frac{1}{2}(Q_t^*Q_{xxt} - Q_tQ_{xxt}^*) - \frac{c\epsilon}{2}(Q_t^*Q_{xxx} - Q_tQ_{xxx}^*) = 0. \end{aligned} \tag{49}$$

By using the identities, the above equation can be represented as

$$\begin{aligned} &i\frac{\partial}{\partial t}|Q_t|^2 - ic^2\frac{\partial}{\partial x}(Q_t^*Q_x + Q_tQ_x^*) + ic^2\frac{\partial}{\partial t}|Q_x|^2 + \frac{1}{2}\left(\frac{\partial}{\partial t}(Q_t^*Q_{xx} - Q_tQ_{xx}^*) - (Q_{tt}^*Q_{xx} - Q_{tt}Q_{xx}^*)\right) \\ &+ (Q_t^*Q - Q_tQ^*)\frac{\partial}{\partial t}|Q|^2 - c\lambda\left(2|Q|^2(Q_t^*Q_x - Q_tQ_x^*) + Q^2Q_t^*Q_x^* - (Q^*)^2Q_tQ_x\right) \\ &- \frac{c\epsilon}{2}\left(\frac{\partial}{\partial x}(Q_t^*Q_{xx} - Q_tQ_{xx}^*) - (Q_{tx}^*Q_{xx} - Q_{tx}Q_{xx}^*)\right) = 0. \end{aligned} \tag{50}$$

The above equation can be written in the conservation law form

$$\frac{\partial T}{\partial t} + \frac{\partial J}{\partial x} = 0, \tag{51}$$

where T and J are as

$$T = i|Q_t|^2 + ic^2|Q_x|^2 + (Q_t^*Q - Q_tQ^*)|Q|^2 + \frac{1}{2}(Q_t^*Q_{xx} - Q_tQ_{xx}^*),$$
$$\text{and } J = -ic^2(Q_t^*Q_x + Q_tQ_x^*) - c\lambda\left(2|Q|^2(Q_t^*Q_x - Q_tQ_x^*) + Q^2Q_t^*Q_x^* - (Q^*)^2Q_tQ_x\right)$$
$$- \frac{c\epsilon}{2}(Q_t^*Q_{xx} - Q_tQ_{xx}^*).$$

Therefore, the conservative quantity from the above equation is written as

$$H = \int_{-\infty}^{\infty}\left(i|Q_t|^2 + ic^2|Q_x|^2 + (Q_t^*Q - Q_tQ^*)|Q|^2 + \frac{1}{2}(Q_t^*Q_{xx} - Q_tQ_{xx}^*)\right)dx, \tag{52}$$

This expression demonstrates the Hamiltonian or conservation of energy for the soliton solutions. The conservation of Hamiltonian proves the physical consistency and stability of the derived solitons.

5.4. Conserved Quantities

From outcome (20), we attained the succeeding conserved quantities as

$$P = \frac{4\omega\sqrt{\mu_2}}{\beta}\left(\nu + \frac{\beta^2}{2}\right),$$
$$M = \frac{2\sqrt{\mu_2}\,\omega}{3\beta^2}\left(12\alpha\mu_2\omega - 3\beta^3 - \beta(\alpha^2\mu_2 + 12\nu)\right),$$
$$H = \frac{2\sqrt{\mu_2}\,\omega}{3\beta^2}\left(3\beta^2(\nu^2 + c^2\beta^2) + 3\alpha^2\mu_2(\nu^2 + c^2\beta^2) - 6\beta^2\nu\alpha\mu_2\omega\right).$$

These conserved quantities prove the physical validity of the obtained soliton solutions and show that the waves possess key dynamical characteristics while propagating in nonlinear dispersive mediums.

6. Bifurcation Analysis

We investigate the bifurcation analysis of the d-mNLSE in this segment. The bifurcation theory explores how small changes in the parameters of the system affect the nature of the solutions, leading to the formation of new equilibrium states or periodic solutions [28]. The stability and diversity of solutions in nonlinear dynamical systems are better understood as a result of this analysis. The second-order ordinary differential equation given in Equation (14) can be written as:

$$A\,\Psi'' + B\,\Psi + C\,\Psi^3 = 0, \tag{53}$$

with coefficients

$$A = \alpha^2\nu + 2\alpha\beta\omega + 2\alpha^2c^2 + 3\alpha^2\beta c\epsilon - 2\omega^2,$$
$$B = 2\nu^2 - \beta^2\nu - 2\beta^2c^2 - \beta^3c\epsilon,$$
$$C = 2(\beta c\lambda + \nu).$$

The real part provides a first integral that determines the allowed integration constant; it does not affect the fixed-point structure of (53). Introducing the parameters

$$p = -\frac{B}{A}, \qquad q = -\frac{C}{A},$$

we obtain the standard Duffing-type oscillator

$$\Psi'' = p\,\Psi + q\,\Psi^3. \tag{54}$$

All subsequent bifurcation analysis is performed on (54), treating p and q as bifurcation parameters.

Equation (54) is rewritten as the first-order system

$$\begin{cases} \Psi' = y, \\ y' = p\,\Psi + q\,\Psi^3. \end{cases}$$

Fixed points satisfy $y = 0$ and $p\,\Psi + q\,\Psi^3 = 0$.

- **Trivial fixed point:** $\Psi_0 = 0$ always exists. Linearization gives the Jacobian matrix

$$J(0,0) = \begin{pmatrix} 0 & 1 \\ p & 0 \end{pmatrix},$$

with eigenvalues $\lambda = \pm\sqrt{p}$.

  - If $p < 0$: eigenvalues are purely imaginary → centre (stable in the linear sense).
  - If $p > 0$: eigenvalues are real of opposite sign → saddle (unstable).
  - If $p = 0$: degenerate (non-hyperbolic).

- **Nontrivial fixed points:** When $p/q < 0$, two additional fixed points appear at

$$\Psi_\pm = \pm\sqrt{-\frac{p}{q}}.$$

Linearization around $\phi_\pm$ yields

$$J = \begin{pmatrix} 0 & 1 \\ p + 3q\Psi_\pm^2 & 0 \end{pmatrix} = \begin{pmatrix} 0 & 1 \\ -2p & 0 \end{pmatrix},$$

because $p + 3q\Psi_\pm^2 = p + 3q(-p/q) = -2p$.

  - If $p < 0$: $-2p > 0 \rightarrow$ real eigenvalues → saddle.
  - If $p > 0$: $-2p < 0 \rightarrow$ purely imaginary eigenvalues → centre.

The existence and stability of the nontrivial points depend on the sign of q:

$q > 0$	$p < 0$	$\Psi_\pm$ exist and are saddles; Ψ_0 is a centre.
	$p > 0$	no nontrivial points; Ψ_0 is a saddle.
$q < 0$	$p < 0$	no nontrivial points; Ψ_0 is a centre.
	$p > 0$	$\Psi_\pm$ exist and are centres; Ψ_0 is a saddle.

At $p = 0$, the trivial fixed point changes stability. The number of fixed points changes from one to three when crossing $p = 0$ (provided $q \neq 0$). This is a **pitchfork bifurcation**.

- For $q > 0$: when p increases through 0, two saddle points annihilate at the origin and the origin turns from a centre into a saddle → **subcritical pitchfork**.
- For $q < 0$: when p increases through 0, two centres appear and the origin changes from a centre to a saddle → **supercritical pitchfork**.

Figure 6 illustrates the fixed-point branches as functions of p for both cases. Panel (a) shows the subcritical case ($q > 0$), where two nontrivial branches exist for $p < 0$ and disappear for $p > 0$. Panel (b) shows the supercritical case ($q < 0$), where two nontrivial branches appear for $p > 0$. The solid line represents the trivial branch $\Psi = 0$, while dashed lines represent the nontrivial branches $\Psi_\pm$.

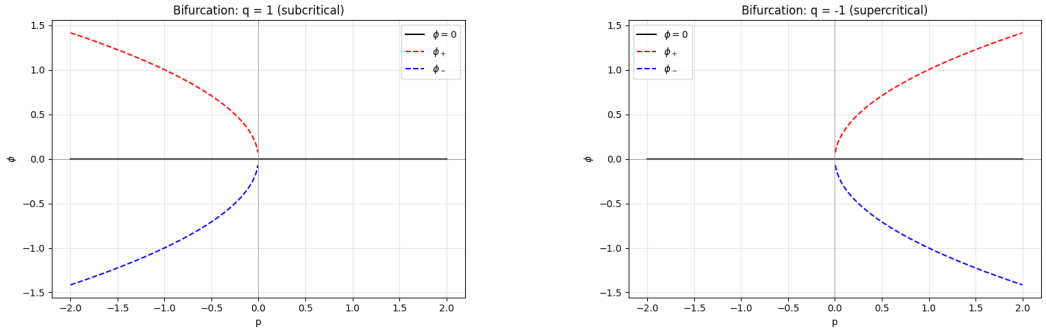
The system derived from the traveling wave reduction is Hamiltonian, with the Hamiltonian function given by

$$H(\Psi, y) = \frac{1}{2}y^2 - \frac{p}{2}\Psi^2 - \frac{q}{4}\Psi^4.$$

Trajectories in the phase plane (Ψ, y) lie on level curves of H. The corresponding potential energy is

$$V(\Psi) = -\frac{p}{2}\Psi^2 - \frac{q}{4}\Psi^4.$$

The nature of the fixed points and the global dynamics depend on the signs of p and q. Figures 7 and 8 illustrate the four characteristic regimes and their associated potential landscapes.

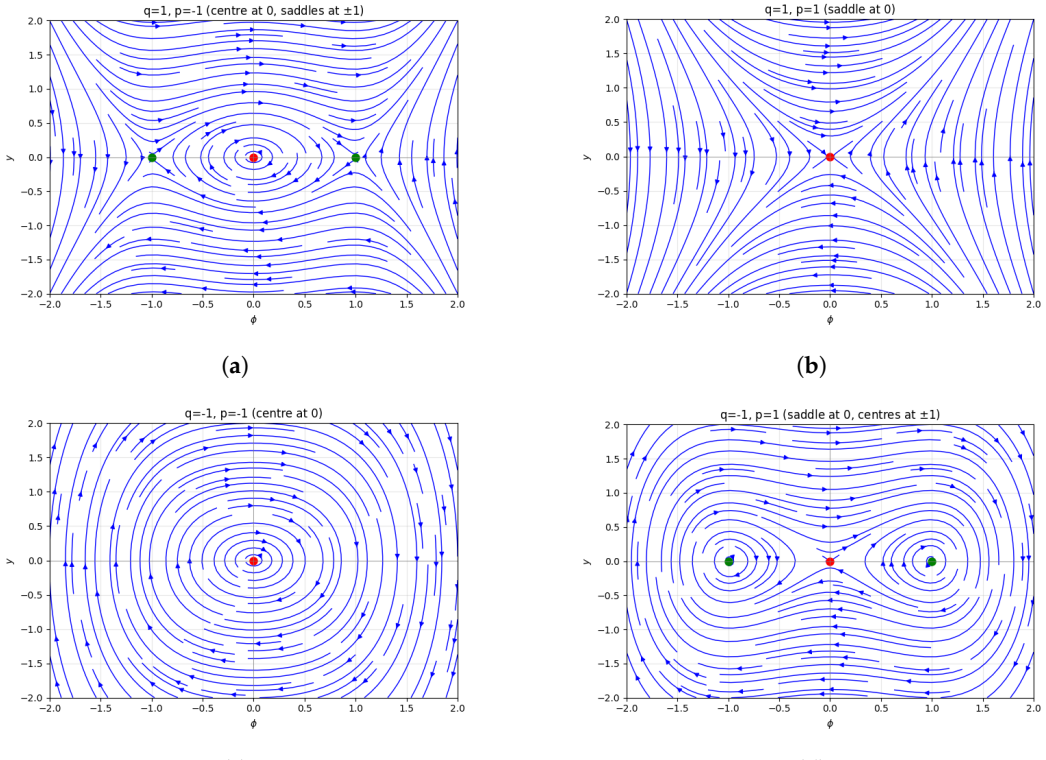


(**a**) (**b**)

Figure 6. Bifurcation diagrams for the d-mNLSE reduction: fixed points ϕ versus parameter p for fixed q. (**a**) Subcritical pitchfork bifurcation ($q > 0$): two saddle points annihilate at $p = 0$. (**b**) Supercritical pitchfork bifurcation ($q < 0$): two centres emerge from $p = 0$.

The bifurcation analysis indicates that the d-mNLSE has an associated pitchfork bifurcation under traveling wave reductions which depend on the parameter p. In addition, the determination of whether the bifurcation is supercritical or subcritical is carried out by the sign of q. This is consistent with conservative systems which represent nonlinearly as cubic (i.e., the type of behavior shown in this analysis). The Python 3.13 code allows visual exploration of the phase space and the bifurcation structure.

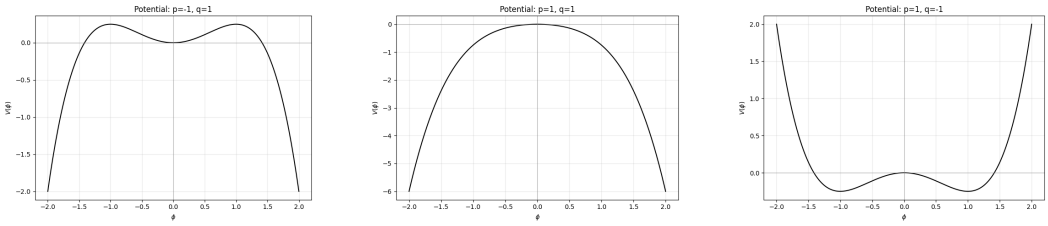
In a physical context, the parameters p and q are related to the wave speed, wave number, frequency, and the intrinsic coefficients λ, ϵ. By varying these physical quantities, one can observe the transition from single-peak to multi-peak wave structures or the appearance of periodic waves.



(**a**) (**b**)

(**c**) (**d**)

Figure 7. Phase portraits of the system $\Psi'' = p\Psi + q\Psi^3$ for the four distinct regimes determined by the signs of p and q. Red dots indicate saddle points, green dots indicate centres. (**a**) Phase portrait for $p < 0,\ q > 0$: centre at $\phi = 0$, saddles at $\Psi = \pm\sqrt{-p/q}$. (**b**) Phase portrait for $p > 0,\ q > 0$: saddle at $\Psi = 0$, no nontrivial fixed points. (**c**) Phase portrait for $p < 0,\ q < 0$: centre at $\Psi = 0$, no nontrivial fixed points. (**d**) Phase portrait for $p > 0,\ q < 0$: saddle at $\phi = 0$, centres at $\Psi = \pm\sqrt{-p/q}$.



(**a**) (**b**) (**c**)

Figure 8. Representative potential landscapes corresponding to different parameter regimes. The potential $V(\Psi) = -\frac{p}{2}\Psi^2 - \frac{q}{4}\Psi^4$ determines the stability of fixed points: minima correspond to centres, maxima to saddles. (**a**) Potential $V(\Psi)$ for $p < 0,\ q > 0$. (**b**) Potential $V(\Psi)$ for $p > 0,\ q > 0$. (**c**) Potential $V(\Psi)$ for $p > 0,\ q < 0$.

7. Physical Insight and Interpretation of the Obtained Results

The analytical solutions attained in this study reveal important physical characteristics of nonlinear wave propagation governed by the d-mNLSE. The hyperbolic and trigonometric solutions represent localized and periodic wave structures arising from the balance among nonlinearity dispersion. In particular, the bright soliton solutions as well as the dark soliton solutions represent the stable localized wave packets that maintain their shapes while propagating through the nonlinear dispersive media. The multi-peak wave solutions as well as the mixed wave solutions imply the possible complex interactions between the dual wave modes. The periodic solutions as well as the mixed periodic solutions imply the possible oscillating wave behavior under certain parameter conditions. In addition to this, the derived CLs for the impulse power, impulse momentum, as well as the impulse energy offer additional physical implications that the derived soliton solutions maintain the fundamental physical properties. The bifurcation analysis again demonstrates the various wave patterns that emerge as the parameters change, showing stability transitions between stable and unstable regimes as well as the creation of additional solution branches through pitchfork bifurcations. The obtained solutions are summarized in Table 1. Therefore, these results influence innate theoretical comprehension of non-linear wave dynamics with potential applications in fluid mechanics, nonlinear optics, plasma physics, and ocean engineering.

Some studies have investigated the d-mNLSE utilizing diverse analytical schemes to attain soliton and wave results. The authors in [20,23] applied the tanh–coth expansion method, the unified Riccati equation method, the modified simple equation method, and the new extended auxiliary equation method to the dual-mode nonlinear Schrödinger equation with Kerr-law nonlinearity in order to derive optical soliton solutions describing solitary wave propagation in dual-mode optical fibers. The authors in [26] used the extended (G'/G)-expansion method to derive optical soliton molecules of the d-NLSE in cubic-law media. In addition, the authors in [16] applied the new extended direct algebraic method to the d-mNLSE to construct exact solutions. Lie symmetry analysis, group-invariant solutions, and conservation laws for the d-mNLSE were studied in [17]. Therefore, compared with previous studies that mainly focused on a limited class of soliton or periodic wave solutions, the present work provides a broader spectrum of analytical solutions and offers a deeper understanding of nonlinear wave dynamics through bifurcation and phase-portrait analysis.

The graphical visualizations (see Figures 1–7), presented through contourplots two- and three-dimensional, and contour plots, further illustrate the propagation characteristics of the obtained solutions. These structures show the amplitude changes, the localization of the wave structures, as well as their evolution in the space. Graphical analysis is an important tool in relating the analytical results to their physical meaning.

Table 1. Comprehensive Classification of Analytical Solutions of the d-mNLSE.

Solution in Equation	Mathematical Form	Wave Profile	Physical Interpretation	Potential Applications
(20)	$\mathrm{sech}(\cdot)$	Bright soliton	Localized pulse with decaying tails	Optical fibers, nonlinear optics
(21)	$\mathrm{csch}(\cdot)$	Singular soliton	Strong localized spike, Wave with central singularity	Plasma waves, nonlinear media
(22)	$\sinh + \cosh$	Shock/kink wave	Rapid transition wave profile	Fluid dynamics, shallow water waves
(23)	$\tanh(\cdot)$	Dark soliton	Intensity dip on background	Bose–Einstein condensates, optics
(24)	$\coth(\cdot)$	Singular dark wave	Dark structure with singularity	Plasma physics
(25)	$\tanh + i\,\mathrm{sech}$	Dark–bright composite soliton	Dual wave interaction	Optical soliton interactions
(26)	$\tanh + \coth$	Mixed hyperbolic	Combined localized structures	Nonlinear dispersive systems
(27)	Hyperbolic ratio	W-shape soliton	Multi-peak localized wave and Energy redistribution among peaks	Pulse shaping
(28)	$\sec(\cdot)$	Periodic singular	Oscillatory singular wave	Ocean waves
(29)	$\csc(\cdot)$	Periodic singular waves	Spatial wave resonance	Surface Water waves
(30)	$\tan(\cdot)$	Periodic wave	Nonlinear oscillation and Energy exchange between wave modes	Nonlinear optics, waveguides
(31)	$\cot(\cdot)$	Periodic singular wave	Periodic wave with Phase-shift oscillation	Waveguide systems, Wave resonance problems
(32)	$\sec - \tan$	Mixed periodic wave	Interaction of periodic components	Nonlinear oscillatory media
(33)	$\tan - \cot$	Combined periodic waves	Multi-mode oscillatory interaction	Optical resonators
(34)	Trigonometric combination	Periodic modulated wave	Modulated wave envelope interaction	Nonlinear signal propagation
(35)	cos / sin	Oscillatory wave	Harmonic nonlinear propagation and wave envelope modulation	Ocean engineering
(36)	Exponential form	Solitary pulse	Localized nonlinear pulse	Optical pulse transmission
(37)	Rational-exponential	Decaying soliton	Asymmetric soliton decay	Plasma wave propagation
(38)	$1/(\zeta + \zeta_0)$	Rational singular solution	Algebraic decay and Strong localized nonlinear interaction	Nonlinear dispersive media
(39)	$1/\sqrt{\zeta + \zeta_0}$	Algebraic wave	Slowly decay with Long-range nonlinear interaction	Fluid mechanics, nonlinear hydrodynamics

8. Conclusions

In the current work, the d-mNLSE is successfully analyzed to understand the dynamics of nonlinear wave interactions during wave propagation in dispersive media. By using the mSS-EM, a wide variety of exact analytical solutions is obtained. The solutions obtained include hyperbolic, trigonometric, periodic, singular, and complex dark–bright soliton structures with multi-peak and mixed wave patterns. These analytical solutions greatly enhance the solution set of the nonlinear model under consideration and provide a deeper understanding of the interaction and evolution of dual-mode wave structures. The achieved solutions may have potential applications in fluid mechanics, nonlinear optics, plasma physics, and ocean engineering, among others, as wave interactions of this kind occur quite frequently in these fields. In addition, the CLs are established for this equation, which lead to the invariant properties such as the impulse power, momentum, and energy of the

soliton structures. These conserved quantities play a critical role in the physical stability of the soliton structures. Furthermore, the qualitative behavior of the mathematical model is analyzed using the bifurcation method for the reduced dynamical system. Equilibrium points are obtained, and the nature of the stability is analyzed, revealing the conditions for the formation of different wave structures. To demonstrate the physical interpretation of the results, graphical representations such as two-dimensional, three-dimensional, and contour plots are obtained, revealing the different propagation characteristics of the obtained wave structures. Moreover, the results demonstrate the efficiency of the suggested analytical method for the construction of soliton solutions for the given nonlinear wave equation.

Author Contributions: M.A., N.N., E.H., M.H. and M.F. contributed equally in this paper. All authors have read and agreed to the published version of the manuscript.

Funding: This research received no external funding.

Data Availability Statement: No new data were created or analyzed in this study. Data sharing is not applicable to this article.

Conflicts of Interest: The authors declare no conflicts of interest.

References

1. Arshad, M.; Shehzad, K.; Bayram, M.; Farman, M.; Sambas, A. Stability, soliton dynamics, and bifurcation analysis of the (3 + 1)-dimensional Sakovich equation in fluid dynamics. *Model. Earth Syst. Environ.* **2025**, *11*, 364. [CrossRef]
2. Mhadhbi, N.; Gana, S.; Alsaeedi, M.F. Exact solutions for nonlinear partial differential equations via a fusion of classical methods and innovative approaches. *Sci. Rep.* **2024**, *14*, 6443. [CrossRef]
3. Ben-Loghfyry, A.; Charkaoui, A. A novel Perona-Malik model driven by fractional regularized diffusion mechanism with caputo derivative applied to magnetic resonance image processing. *J. Frankl. Inst.* **2025**, *362*, 107950. [CrossRef]
4. Kopçasız, B.; Yaşar, E. Inquisition of optical soliton structure and qualitative analysis for the complex-coupled Kuralay system. *Mod. Phys. Lett. B* **2025**, *39*, 2450512. [CrossRef]
5. Murad, M.A.S. Soliton solutions of cubic quintic septimal nonlinear Schrödinger wave equation with conformable derivative by two distinct algorithms. *Phys. Scr.* **2024**, *99*, 105247. [CrossRef]
6. Ahmed, K.K.; Ahmed, H.; Badra, N.M.; Mirzazadeh, M.; Rabie, W.B.; Eslami, M. Diverse exact solutions to Davey–Stewartson model using modified extended mapping method. *Nonlinear Anal. Model. Control* **2024**, *29*, 983–1002. [CrossRef]
7. Shahen, N.H.M.; Rahman, M.M.; Alshomrani, A.S.; Inc, M. On fractional order computational solutions of low-pass electrical transmission line model with the sense of conformable derivative. *Alex. Eng. J.* **2023**, *81*, 87–100. [CrossRef]
8. Iqbal, M.A.; Miah, M.M.; Ali, H.S.; Shahen, N.H.M.; Deifalla, A. New applications of the fractional derivative to extract abundant soliton solutions of the fractional order PDEs in mathematics physics. *Partial Differ. Equ. Appl. Math.* **2024**, *9*, 100597. [CrossRef]
9. Yasin, F.; Shahbaz, N.; Almutairi, B.; Sesay, M.; Macías-Díaz, J.E. Exploring soliton solutions of Zakharov–Kuznetsov dynamical model with applications. *AIP Adv.* **2025**, *15*, 045212. [CrossRef]
10. Kopçasız, B.; Sağlam, F.N.K.; Malik, S. Exact soliton solutions for the (n + 1)-dimensional generalized Kadomtsev–Petviashvili equation via two novel methods. *Int. J. Geom. Methods Mod. Phys.* **2025**, *22*, 2550105. [CrossRef]
11. Rogers, C.; Schief, W.K. *Bäcklund and Darboux Transformations: Geometry and Modern Applications in Soliton Theory*; Cambridge University Press: Cambridge, UK, 2002; Volume 30.
12. Sağlam, F.N.K.; Kopçasız, B.; Şenol, M. Abundant new soliton solutions to the Arshed–Biswas equation via two novel integrating schemes. *Mod. Phys. Lett. A* **2025**, *40*, 2550054. [CrossRef]
13. Kopçasız, B.; Yaşar, E. μ-Symmetries and μ-Conservation Laws for The Nonlinear Dispersive Modified Benjamin-Bona-Mahony Equation. *J. Math. Sci. Model.* **2023**, *6*, 87–96. [CrossRef]
14. Mahmood, S.S.; Murad, M.A.S. Analytical Soliton Solutions to the Dual-Mode Fourth-Order Nonlinear Schrödinger Equation Governed by a Parabolic Law. *J. Exp. Theor. Phys.* **2025**, *141*, 22–31. [CrossRef]
15. Omar, F.M.; Murad, M.A.S. Soliton solutions, bifurcation analysis, and chaos in the dual-mode conformable nonlinear Schrödinger equation with generalized power-law nonlinearity. *Nonlinear Dyn.* **2025**, *113*, 33735–33755. [CrossRef]
16. Kopçasız, B.; Yaşar, E. Novel exact solutions and bifurcation analysis to dual-mode nonlinear Schrödinger equation. *J. Ocean Eng. Sci.* **2022**. [CrossRef]
17. Kopçasız, B.; Yaşar, E. Dual-mode nonlinear Schrödinger equation (DMNLSE): Lie group analysis, group invariant solutions, and conservation laws. *Int. J. Mod. Phys. B* **2024**, *38*, 2450020. [CrossRef]

18. Alam, B.E.; Javid, A. Optical dual-waves to a new dual-mode extension of a third order dispersive nonlinear Schrödinger's equation. *Phys. Lett. A* **2023**, *480*, 128954. [CrossRef]
19. Rehman, H.U.; Khushi, K.; Iqbal, I.; Sherif, E.S.M.; Shahzad, M.U.; Khan, M.A. Analysis of optical solitons propagation in the dual-mode resonant nonlinear Schrödinger dynamical equation with assorted nonlinear interactions. *Mod. Phys. Lett. B* **2025**, *39*, 2450433. [CrossRef]
20. Jaradat, I.; Alquran, M.; Momani, S.; Biswas, A. Dark and singular optical solutions with dual-mode nonlinear Schrödinger's equation and Kerr-law nonlinearity. *Optik* **2018**, *172*, 822–825. [CrossRef]
21. Wazwaz, A.M. Two-mode Sharma-Tasso-Olver equation and two-mode fourth-order Burgers equation: Multiple kink solutions. *Alex. Eng. J.* **2018**, *57*, 1971–1976. [CrossRef]
22. Javid, A.; Seadawy, A.R.; Raza, N. Dual-wave of resonant nonlinear Schrödinger's dynamical equation with different nonlinearities. *Phys. Lett. A* **2021**, *407*, 127446. [CrossRef]
23. Zayed, E.M.; Shohib, R.M. Optical solitons and other solutions to the dual-mode nonlinear Schrödinger equation with Kerr law and dual power law nonlinearities. *Optik* **2020**, *208*, 163998. [CrossRef]
24. Xiao, Z.J.; Tian, B.; Zhen, H.L.; Chai, J.; Wu, X.Y. Multi-soliton solutions and Bäcklund transformation for a two-mode KdV equation in a fluid. *Waves Random Complex Media* **2017**, *27*, 1–14. [CrossRef]
25. Jaradat, H.M.; Syam, M.; Alquran, M. A two-mode coupled Korteweg–de Vries: Multiple-soliton solutions and other exact solutions. *Nonlinear Dyn.* **2017**, *90*, 371–377. [CrossRef]
26. Kopçasız, B.; Seadawy, A.R.; Yaşar, E. Highly dispersive optical soliton molecules to dual-mode nonlinear Schrödinger wave equation in cubic law media. *Opt. Quantum Electron.* **2022**, *54*, 194. [CrossRef]
27. Borhan, J.R.M.; Mamun Miah, M.; Duraihem, F.Z.; Iqbal, M.A.; Ma, W.X. New optical soliton structures, bifurcation properties, chaotic phenomena, and sensitivity analysis of two nonlinear partial differential equations. *Int. J. Theor. Phys.* **2024**, *63*, 183. [CrossRef]
28. Kopçasız, B.; Yaşar, E. Soliton solutions, sensitivity analysis, and multistability analysis for the modified complex Ginzburg-Landau model. *Eur. Phys. J. Plus* **2025**, *140*, 216. [CrossRef]
29. Zhang, J.B.; Ma, W.X. Mixed lump-kink solutions to the BKP equation. *Comput. Math. Appl.* **2017**, *74*, 591–596. [CrossRef]
30. Ashaq, H.; Majid, S.Z.; Riaz, M.B.; Asjad, M.I.; Muhammad, T. Exploring optical solitary wave solutions in the (2 + 1)-dimensional equation with in-depth of dynamical assessment. *Heliyon* **2024**, *10*, e32826. [CrossRef]
31. Korsunsky, S.V. Soliton solutions for a second-order KdV equation. *Phys. Lett. A* **1994**, *185*, 174–176. [CrossRef]
32. Hirota, R.; Satsuma, J. Soliton solution of the coupled KdV system. *Phys. Lett. A* **1981**, *85*, 407–408. [CrossRef]
33. Raza, N.; Jhangeer, A.; Arshed, S.; Butt, A.R.; Chu, Y.M. Dynamical analysis and phase portraits of two-mode waves in different media. *Results Phys.* **2020**, *19*, 103650. [CrossRef]

Disclaimer/Publisher's Note: The statements, opinions and data contained in all publications are solely those of the individual author(s) and contributor(s) and not of MDPI and/or the editor(s). MDPI and/or the editor(s) disclaim responsibility for any injury to people or property resulting from any ideas, methods, instructions or products referred to in the content.